Journal Name

ARTICLE

Glyco-functionalized dinuclear rhenium(I) complexes for cell imaging

Received 00th January 20xx,
Accepted 00th January 20xx

DOI: 10.1039/x0xx00000x

www.rsc.org/

Alessandro Palmioli,[a,e] Alessandro Aliprandi,[b] Dedy Septiadi,[b] Matteo Mauro*[b], Anna Bernardi,[a] Luisa De Cola[b], Monica Panigati,*[a,c,d]

The design, synthesis and photophysical characterization of four new luminescent glycosylated luminophores based on dinuclear rhenium complexes, namely Glyco-Re, is described. The derivatives have general formula $[Re_2(\mu\text{-}Cl)_2(CO)_6(\mu\text{-}pydz\text{-}R)]$ (R-pydz = functionalized 1,2-pyridazine), where a sugar residue (R) is covalently bound to the pyridazine ligand in the β position. Different synthetic pathways have been investigated including the so-called neo-glycorandomization procedure, affording stereosectively glyco-conjugates containing glucose and maltose in β anomeric configuration. A multivalent dinuclear rhenium glycodendron bearing three glucose units is also synthesized. All the Glyco-Re conjugates are comprehensively characterized and their photophysical properties and cellular internalization experiments on human cervical adenocarcinoma (HeLa) cells are reported. The results show that such Glyco-Re complexes display interesing bio-imaging properties, i.e. high cell permeability, organelle selectivity, low cytotoxicity, fast internalization. These findings make the presented Glyco-Re derivatives efficient phosphorescent probes suitable for cell imaging application.

Introduction

Carbohydrates play a crucial role in different important biological processes such as cell proliferation and differentiation as well as cellular immune response. Therefore monitoring their uptake process and distribution inside cellular compartments is of fundamental importance for the diagnosis of various diseases and for developing new therapeutic agents.[1]

Luminescent organometallic complexes based on second and third row transition metals possess unique spectroscopic and photophysical properties, such as high emission quantum yield, photostability and long-lived excited states and sensitivity to the local surrounding. Nowadays, all these features have been advantageously employed for bio-imaging purposes and this research topic is attracting a very much deal of attention due to the potential scientific fall-outs in biology, bio-chemical and medical research. [2] Moreover, metal complexes could be endowed with high photoluminescence quantum yields even in air-equilibrated aqueous media and relatively long lifetimes by proper molecular design. Furthermore, they may exhibit low toxicity and good cellular internalization features.[3]

In this respect, combining biomolecules, such as carbohydrates, with transition-metal complexes to generate luminescent bioconjugates represents a promising strategy to obtain sensitive molecular tools to gain deeper insight into biological key-event such as cellular internalization processes, metabolism and biodistribution.

Due to their high water solubility, carbohydrates can be favorably used to effectively solubilize apolar structures in polar media. Furthermore, it is now well established that carbohydrates are involved in a variety of molecular recognition phenomena of physiological and pathological relevance in living organisms that could be imaged using glycosylated luminescent probes1[b].

Various luminescent transition-metal glycoconjugate complexes based on ruthenium(II), [4] iridium(III) [5] and platinum(II)[6] have been recently reported and amongst them phosphorescent rhenium(I) tricarbonyl polypyridine complexes are the most extensively studied systems.

Although the use of the rhenium(I) glyco-conjugates as biosensors in carbohydrate-related events goes back to 2006,[7] quite surprisingly their application as luminescent probes for cell imaging has been little exploited to date. Indeed, only three examples have been reported so far in the literature, to the best of our knowledge.[8] Such examples deal with

[a] Department of Chemistry, Università degli Studi di Milano, Via Golgi 19, 20133 Milano (Italy). Fax: +39 0250314405; Tel: +30 0250314352; E-mail: monica.panigati@unimi.it
[b] ISIS & icFRC, Université de Strasbourg & CNRS, 8 rue Gaspard Monge, 67000 Strasbourg, France, e-mail: mauro@unistra.fr.
[c] Milan Unit of INSTM, Via Golgi 19, 20133 Milano (Italy).
[d] Istituto per lo Studio delle Macromolecole, Consiglio Nazionale delle Ricerche (ISMAC-CNR), Via E. Bassini, 15, 20133 Milano, Italy
[e] Present address: Università degli Studi di Milano-Bicocca, Dipartimento di Biotecnologie e Bioscienze, Piazza della Scienza 2, 20126 Milano, Italy

Electronic Supplementary Information (ESI) available: See DOI: 10.1039/x0xx00000x

mononuclear cationic complexes, containing aromatic either bipyridyl (bpy) or dipyridophenazine (dppz) ligands, which show cytotoxic activity with IC_{50} value in the low micromolar range.

In last few years our groups have developed a novel family of neutral dinuclear rhenium(I) derivatives (see Chart 1) that exhibits intense emission in the visible region, originating from a triplet-manifold excited state being a metal-to-ligand charge transfer (^{3}MLCT) in nature. These neutral derivatives, which can be obtained with good reaction yields, are characterized by two $Re(CO)_3$ units connected by a substituted diazine ligand and two anionic ancillary ligands.[9] Also, modulation of the photophysical properties was promptly achieved by both substituent effect on the diazinic moiety and ancillary bridging ligands, reaching photoluminescence quantum yield values, (Φ), as high as 0.53, when electron-rich diazine ligands were employed and chlorine chosen as the bridging ligand (X = Cl).[10]

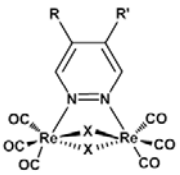

Chart 1 General structure of dinuclear Re(I)-complexes bearing a bridging 1,2-diazine ligands with different alkyl groups (R and R') and two ancillary anionic ligands (X = Cl, Br, I).

Owing to their highly interesting photophysical features and photostability, including high Φ and the possibility to stimulated them by two-photon excitation techniques, this family of dinuclear complexes have been used as low-toxicity luminescent tags for Peptido Nucleic Acids (PNAs) labelling, and successfully tested in cell imaging experiments[11], showing negligible cytotoxicity and efficient cell uptake in living cells with different kinetics and localization depending on the nature of the PNA chain and of the diazine substituent. The stiff "$Re(\mu\text{-}Cl)_2Re$" skeleton, which leads to high photoluminescence quantum yields in solution, allowed imaging at low concentration (25-100 μM), and prevented the release of the chlorides ligands which was often responsible for the toxicity as reported for neutral monuclear diimine rhenium chloride complexes.[12]

These results prompted us to investigate the possibility to develop new luminescent labels for novel glycosylated probes based on these dinuclear rhenium complexes as simple, chemically robust, and easy-to-synthetize platforms that can accommodate different carbohydrates.

Using the synthetic approach of the neo-glycorandomization technique, [13] which allows the direct functionalization of unprotected sugars in the anomeric positions, a series of luminescent glyco-functionalized neutral dinuclear rhenium complexes is prepared. Hereafter, the effects of substituents bound to the diazine ligand, length of the spacer, as well as nature and number of the conjugated carbohydrates on the photophysical properties is reported. Finally, the intracellular distribution of the complexes by means of laser scanning confocal fluorescent microscopy will be discussed.

Result and Discussion

Design and synthesis

Two different dinuclear rhenium complexes (see Chart 2) were selected as starting materials for the synthesis of glyco-Re derivatives **3**-**6** aiming to study their solubility, the photophysical behavior and the cellular uptake of these new glycoconjugates (see Chart 3). Indeed, length, degree of branching and the flexibility of the spacer could be important to control the affinity of the resulting conjugate with the cell surface receptors. Furthermore, number and type of connected sugars, as well as the chemical and biological stability of the linker moiety are also crucial factors to consider in the design of the bio-conjugated luminophores.

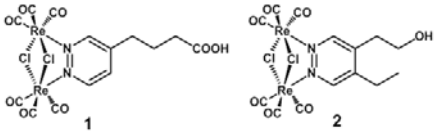

Chart 2 The dinuclear Re complexes **1** and **2** used as luminescent labels.

Complex **1** was already used as luminescent probe for PNA labelling[11,16] while the new complex **2**, which contains two alkyl substituents in the β positions of the diazine ring, could provide blue shifted emission, with higher quantum yield and longer lifetime compared to the analogous mono-substituted complex **1**.[10,15] Both the complexes were synthetized using the previously reported two-steps procedure involving an inverse-type [4+2] Diels–Alder cycloaddition reaction between the electron-poor 1,2,4,5-tetrazine and the appropriate functionalized alkynes with N_2 loss.[14] Following our previously reported procedure,[9,14] the complexes **1** and **2** were prepared by refluxing $[Re(CO)_5Cl]$ with 0.5 equivalents of the corresponding 1,2-diazine in toluene solution.

Formattato: Apice

Formattato: Apice

Formattato: Apice

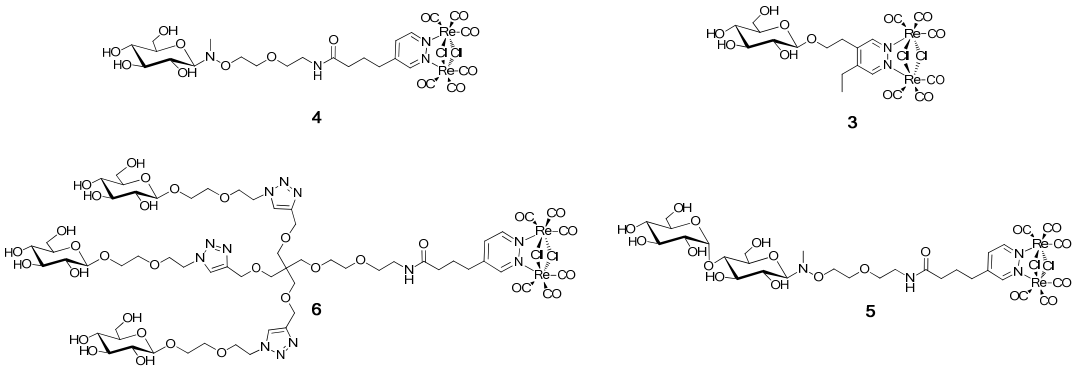

Chart 3 Structure of neutral dinuclear Re-glycoconjugates **3**-**6** synthesized in this study.

Complex **3**, consisting of a β-*O*-glucoside derivative of the dinuclear rhenium complex **2**, was synthetized as shown in Scheme 1. Commercial hex-3-ynol **7** was glycosylated with penta-*O*-acetyl-D-glucose **8** and the resulting product **9** was deacetylated under Zemplen condition, obtaining the β-hex-3-ynyl-1-*O*-β-D-glucopyranoside-alkyne **10**. Alkyne **10** was used for the synthesis of the diazine ligand, following the well-established literature procedure involving an inverse-type [4 + 2] Diels-Alder cycloaddition reaction between the electron-poor 1,2,4,5-tetrazine and the alkyne dienophile, that occur with N_2 loss.[14,19] Finally, the functionalized diazine ligand (**11**) was treated with two equivalents of the organometallic precursor $Re(CO)_5Cl$ obtaining the final β-*O*-D-glucoside-Re complex **3**. Both **3** and the corresponding diazine ligand **11** were isolated and purified by reverse phase chromatography. Complex **3** was isolated as a yellow solid which was found to be soluble at mM level in organic polar solvents, such as MeOH and DMSO, and in a 1:1 MeOH:H_2O mixture. Although all synthetic intermediates and final compounds have been successfully isolated and fully characterized, this synthetic strategy has poor overall yield, principally because of the two last steps, which have reaction yield of 35% and 12%, respectively.

Formattato: Apice

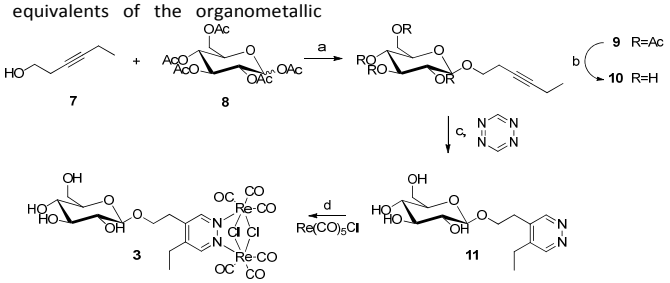

Scheme 1 Schematic synthetic pathway employed for preparing compound **3**. Reagents and conditions: a) $BF_3{\cdot}Et_2O$, CH_2Cl_2 dry, 0 °C then room temperature, 4 hours, yield 53%; b) NaOMe 0.1 M, MeOH dry, room temperature, 1 hour, yield 81%; c) 1,4-dioxane, 80 °C, 24 hours, yield 35%; d), toluene, reflux, 3 hours, yield 12%.

For this reason the synthetic procedure shown in Scheme 1 was not suitable for the synthesis of a large set of conjugates containing different natural monosaccharides and oligosaccharides. Therefore a bifunctional linker (**16**, see Scheme 2), that bears a primary amino group and an *N*-methylamino-oxy group was developed. It could act as a robust and easily accessible platform, able to accommodate both the photoluminescent tag and the different carbohydrate moieties in a fast, convergent and parallel way. This linker allowed exploiting the chemoselective glycosylation approach based on the one-step reaction of *N*-methylamino-oxy groups with an unprotected non-activated reducing sugar, affording a neo-glycoconjugate under mild conditions. [15] In addition, the formed neo-glycosidic linkage was quite stable in physiological condition and toward enzymatic hydrolysis. Overcoming protection/activation/deprotection steps of traditional glycosylation reactions, this method was used for the preparation of the glyco-conjugates **4** and **5** as reported in Scheme 2.

Journal Name

ARTICLE

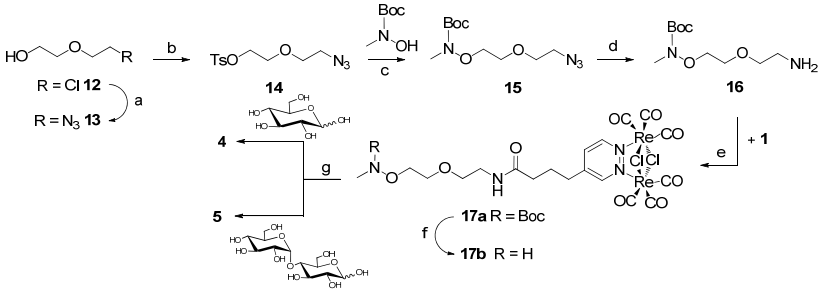

Scheme 2 Schematic synthetic pathways employed for the neoglyco-conjugates **4** and **5**. Reagents and conditions: a) NaN_3, NaI, H_2O, 60 °C, 4 days, quantitative yield; b) TsCl, Et_3N, DCM, 0 °C then room temerature, 3 hours, yield 80%; c) 1,5-diazabiciclo(5.4.0)undec-5-ene (DBU), THF then solvent-free, room temperature, 12 hours, yield 88%; d) PPh_3, Na_2CO_3, H_2O, CH_2Cl_2, room temperature, 12 hours, yield 85%; e) HATU, DIPEA, CH_2Cl_2 (5% dry DMA), room temperature, 2 hours, yield 76%; f) TFA, dry CH_2Cl_2, 1 hour, quantitative yield; g) D-glucose or maltose, glacial AcOH, dry MeOH, room temperature, 18 hours, yield 62% and 63% for **4** and **5**, respectively.

The 2-(2-azidoethoxy) ethanol (**13**, obtained from commercial 2-(2-chloroethoxy) ethanol (**12**) and NaN_3 (Scheme 2), was first tosylated (14) and then treated with *N*-Boc-*N*-methylhydroxylamine and DBU to afford *N*-Boc-*N*-methyl-2-(2-azidoethoxy)ethoxy hydroxylamine (**15**). Then the azido group was reduced under Staudinger condition (PPh_3 and water) and the amine **16** was coupled with dinuclear Re(I) complex **1** affording the intermediate **17a** with satisfactory overall yield. The *N*-Boc protecting group was removed in the presence of CF_3COOH in CH_2Cl_2 and the resulting *N*-methyl hydroxylamine **17b** was isolated as the trifluoroacetate salt in quantitative yield. Finally, chemoselective glycosylation of **17b** to afford **4** or **5** was performed in the presence of 3 eq. of unprotected reducing sugar (D-glucose or D-maltose, respectively) and 25 eq. of AcOH in MeOH at room temperature overnight (Scheme 2). The neo-glycoconjugate products were obtained stereoselectively in β anomeric configuration with satisfactory yields (62% and 63% for **4** and **5**, respectively). Compounds **4** and **5** are both soluble in water in low mM range concentration.

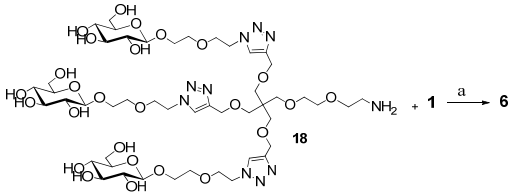

Scheme 3 Synthesis of the multivalent glycoconjugate **6**. Reagents and conditions: a) **1**, HATU, DIPEA, dry DMA, room temperature, 2 hours, yield, 2h, 68%

Finally, for the synthesis of the multivalent glycoconjugate **6** (Scheme 3), the trivalent glucodendron **18** was prepared from commercial pentaerythritol (the full synthetic scheme is reported Scheme S1 of the Electronic Supplementary Information) and linked with the dinuclear Re(I) complex **1** using HATU/DIPEA as coupling reagents. The Re(I)-glycodendrimer **6** was purely isolated after reverse-phase C18 chromatography purification. Complex **6** was soluble in water in mM concentration.

Photophysical characterization

The photophysical properties of the glyco-derivatives **3**-**6** and of their parent complexes **1** and **2** were studied in diluted (concentration of $1.0x10^{-5}$ M) both air-equilibrated and de-areated 1,4-dioxane solutions at room temperature. The multi-functionalized complex **6** was investigated in water solution due to its very low solubility into apolar solvents. The corresponding photophysical data are listed in Table 1.

At longer wavelengths, the electronic absorption spectra of compounds **1–5** in dioxane display broad absorption band with maxima in the range 347–359 nm with moderate intensity ($\varepsilon \approx 0.67–0.88 \times 10^4$ M^{-1} cm^{-1}), whilst complex **6** in distilled H_2O displays an absorption maximum centred at $\lambda_{abs} = 323$ ($\varepsilon \approx 0.55 \times 10^4$ M^{-1} cm^{-1}). Such transition can be assigned to the spin allowed $d\pi(Re) \rightarrow \pi^*$(diazine ring) ^{1}MLCT band as typical of this class of complexes.[9,10] Also, the CT character of such transitions was supported by the modulation effect on the absorption energy, by both the substituents on the diazine ligand and the solvent polarity. Accordingly, complexes **2** and **3**, featuring a diazine containing two alkyl substituents in the β positions, displayed a blue-shifted absorption band, with

Formattato: Apice

respect to the mono substituted complexes **1**, **4** and **5**. Indeed, the second electro-donating alkyl chain on the diazine ligand increases the energy level of the LUMO, raising in this way the HOMO-LUMO gap and therefore the energy of the ^{1}MLCT excited state.[10,15] A hypsochromically shifted absorption band was also observed for complex **6** but, in this case, this feature is most likely due to the much higher polarity of solvent used (water *vs.* dioxane). It is interesting to note that the conjugation of carbohydrate on the organometallic scaffold does not modify the absorption properties, as previously observed also for the analogous for PNA-conjugates.[11,16]

Table 1 Photophysical properties obtained for compounds **1**–**6** in both air-equilibrated and deaerated dilute samples at room temperature.

Compound		λ_{abs} (ε) (nm, [$\times10^4$ $M^{-1}cm^{-1}$])	λ_{em} [nm]	τ [μs]	Φ_{em} (%)	k_r [$\times10^5$ s^{-1}]	k_{nr} [$\times10^5$ s^{-1}]
1[a]	air	359 (0.76)	585	0.378	3		
	deg	-	585	1.27	8	0.63	7.24
2[a]	air	348 (0.88)	562	0.458	3		
	deg	-	562	3.26	20	0.61	2.45
3[a]	air	347 (0.70)	570	0.451	3		
	deg	-	570	2.73	19	0.68	2.98
4[a]	air	352 (0.67)	591	0.419	3		
	deg	-	588	1.18 (81%), 1.83 (19%)	7.2	0.55	7.13
5[a]	air	355 (0.77)	589	0.436	4		
	deg	-	589	1.36	11	0.78	6.36
6[b]	air	323 (0.55)	594	0.011 (17%), 0.144 (74%), 0.504 (9%)	<1		
	deg	-	594	0.365 (24%), 0.138 (38%), 0.014 (38%)	<1	0.66	66.0

[a] in 1,4-dioxane; [b] in distilled water;

Upon excitation in the range 350–380 nm at room temperature, all the samples showed broad and featureless emission in the yellow-orange region of the visible spectrum, which is assigned to the radiative decay of the ^{3}MLCT excited state, as comparison with closely related complexes (see Fig. 1).[10,15] In addition, the triplet nature of the radiative transition is further supported by the oxygen quenching effect observed going from degassed to air-equilibrated samples (Table 1). Similarly to what observed in the absorption spectra, complex **1** and its related glyco-conjugates **4**–**5** display remarkably different emission features compared to derivatives **2**–**3**.

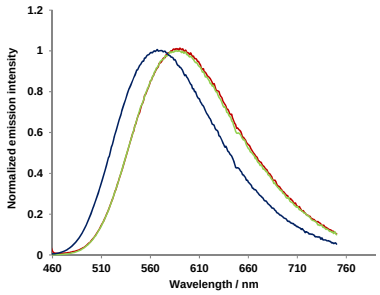

Fig. 1 Normalized emission spectra of complexes **3** (blue trace), **4** (red trace) and **5** (green trace) in deaerated 1,4-dioxane solution at concentration of 1.0×10^{-5} M at room temperature (λ_{ex} 380-400 nm).

Indeed, a hypsochromically shifted and more intense emission was recorded for complexes **2**–**3,** which is accompanied by a higher Φ and longer emission lifetime as consequence of the higher energy of the ^{3}MLCT excited state (see Table 1). However, for all the complexes the values of Φ/τ, which represents the product between the radiative rate constant (k_r) and the efficiency of intersystem crossing (η_{ICS}), were found in the range of 6.1–8.4×10^4 s^{-1}, indicating that the differences observed in the luminescence properties are to be attributed to the nonradiative processes, k_{nr}.

Even if the conjugation with sugar is not expected to modify the nature of the excited state, it is interesting to note that deareated Φ and excited-state lifetime for the glyco-substituted complex **3** were slightly lower than those observed for the non-functionalized benchmark complex **2**. The reason can be likely ascribed to the increased conformational freedom due to the presence of the glucose moiety, which may favour nonradiative deactivation pathways as suggested by the moderate increase of the k_{nr} for complex **3** (see Table 1). The same behaviour was observed for complex **4**, in comparison with the model complex **1**, while complex **5** showed a higher quantum yield and a longer and bi-exponential decay (also observed for complex **4**). This feature is most likely attributed to the formation of soft supramolecular aggregates by establishment of sugar-sugar interactions due to the amphiphilic nature of complexes **4** and **5** upon freeze-pump procedure. The simultaneous presence of the apolar head core, constituted by the dinuclear rhenium complex, and the

hydrophilic sugar moiety, connected to each other by a flexible hydrophilic chain, is expected to promote self-organization of the molecules in solution, as recently reported by some of us.[16] It is reasonable to think that such self-assembling process is further driven by intermolecular hydrogen bonds between the hydroxyl groups of the glucose and maltose moieties in an apolar media such as dioxane, affording large vesicular-like structures in which the apolar "$Re(CO)_3$" heads are oriented towards dioxane solvent media. The formation of such soft aggregates in which phosphorescent $[Re_2(\mu\text{-}Cl)_2(CO)_6(\mu\text{-}pydz)]$ moieties are in close proximity to each other might be responsible of the observed decrease of Φ and bi-exponential character of τ for derivative **4** with respect to the parental complex **1**.

On the other hand, diluted samples of complex **6** in distilled H_2O display rather low photoluminescence with λ_{em} centred at 594 nm and rather short-lived lifetimes even after degassing procedure. This finding is attributed to the large increase of radiationless decay channels as demonstrated by the high k_{nr} constant as consequence of the detrimental aggregation of such amphiphilic derivatives in aqueous media.

The aggregation behaviour of **4** and **5** was also investigated with ^{1}H-NMR spectroscopy in d_4-methanol solution at room temperature. In the ^{1}H-NMR spectra of diluted solution of either **4** or **5** (1 mM) no resonance signal of the N–*H* proton of the amide group of the linker was observed, due to the H-D exchange with the solvent. However, upon increasing the concentration of the complex, up to 20 mM, the rise of a triplet signal at about 8.00 ppm, attributed to the N–*H* involved into stable intermolecular *H*-bond interactions, was observed (see Fig. 2).

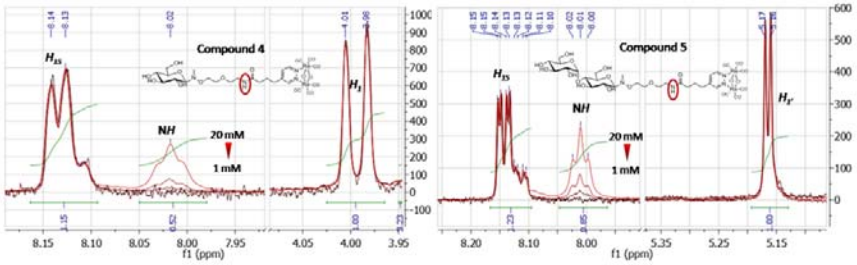

Fig. 2 ^{1}H-NMR spectra recorded for compound **4** and **5** in methanol-d_4 at concentration range from 1 to 20 mM at room temperature. The red symbol shows the variation of the resonance upon increase of the concentration.

Cellular uptake assays

In order to study the internalization and bio-imaging properties of the glyco-Re(I) complexes as cellular probes, we performed cellular uptake experiments of complexes **3**–**6** on human cervical carcinoma (HeLa) cell line. As depicted in Fig. 3, compound **3** was internalized by living HeLa cells and accumulates mainly in the cytoplasmic region with corresponding intracellular emission was centred at 573 nm, as previously observed from photophysical measurements in solution. Complex **4**–**5** display efficient internalization into HeLa cells as well. In order to understand the effect of initial concentration of staining complexes on the cellular behaviour at a specific incubation time, we carried out concentration dependent uptake experiments. Expectantly, increasing the concentration of the staining solution from 25 to 100 µM

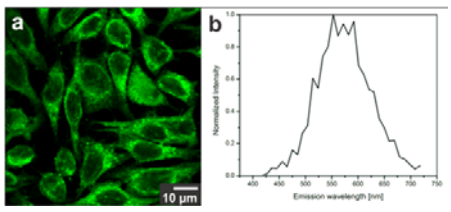

Fig. 3 (a) Fluorescence confocal image of HeLa cells after the incubation of the compound 3 (50 µM in less than 1% DMSO containing PBS). (b) The emission spectrum recorded from the cytoplasm of the cells. The samples were excited at λ_{exc} = 405 nm.

results in an increase of the numbers of internalized molecules as can be noticed through increments of emission intensity signals (see Fig. 4 for compound **4** and Fig. S3 for compound **5**; see also corresponding intensity profile for compound **4** in Fig. S4 of the ESI). We also found that there is no significant difference in term of intracellular distribution of the complexes since for example migration of the complexes towards the nuclear region was not observed at higher concentration (100 µM). Moreover, by means of a live cell imaging technique, we were able to follow in real-time the kinetics of internalization of our compounds. We found out that the uptake of compound **3** as an example, occurred in a short time. Low intensity signal can be observed just a few seconds after the incubation while intense staining patterns can be clearly seen from cytoplasmic region of the cells after 10 min of incubation and they increased over time for 1 hour (Fig. 5, complex **3**). We also observed a similar trend for compound **4** and **5** (see Fig. S5 and S6 respectively). By comparing the intensity profile over time for all of the complexes, we found out that emission signal for cells stained with complex **5** show the highest progression at each acquisition times. Such finding may

underline a faster internalization of compound **5** compared to compound **3** and **4**, by keeping in mind that experimental condition were kept the same and the photophysical properties of the three complexes, especially in term of luminescence quantum yield are comparable (see Fig. S4 and photophysical data listed in Table 1). The higher cellular uptake of the more hydrophilic complex **5** could be most likely associated with an active transport mechanism, which should be further investigated.

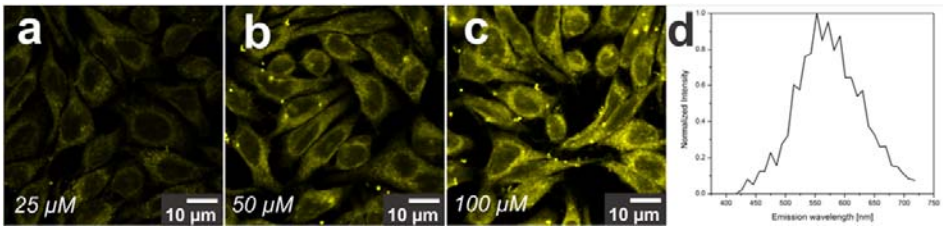

Fig. 4 Confocal images of HeLa cells after the incubation of the compound **4** at different concentrations (a) 25, (b) 50, and (c) 100 μM in less than 1% v/v DMSO containing PBS. (d) The emission spectrum recorded from the cytoplasmic region of the cell. The samples were excited at λ_{exc} = 405 nm.

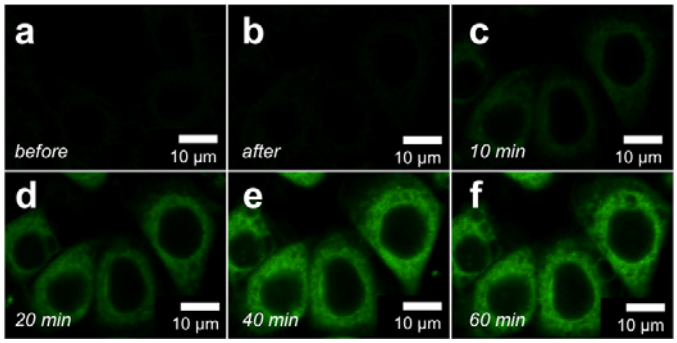

Fig. 5. Confocal images of HeLa cells line (a) before and (b-f) after addition of the compound **3** at concentration 100 μM in less than 1% v/v DMSO containing PBS. Kinetics experiment shows fast internalization of compound at different time (b) seconds, (c) 10 minutes, (d) 20 minutes, (e) 40 minutes, and (f) 1 hour after incubation. The samples were excited at λ_{exc} = 405 nm.

Furthermore, co-localization experiments were performed by co-staining with DAPI (nucleus staining), ER-Tracker™ Red (endoplasmic reticulum staining) and Alexa Fluor® 647 Phalloidin dyes (F-actin staining). As displayed in Fig. 6a-d, results obtained with DAPI co-staining, excluded the presence of all complexes inside the nuclear region whereas a perfect overlapping with signals derived from ER-Tracker™ Red was shown, indicating its co-localization (with overlap coefficient 0.87) in endoplasmic reticulum (Fig. 6e-g). Same results were also obtained for compound **3** and **5**, as shown in Fig. S7 and S8 in the Electronic Supplementary Information.

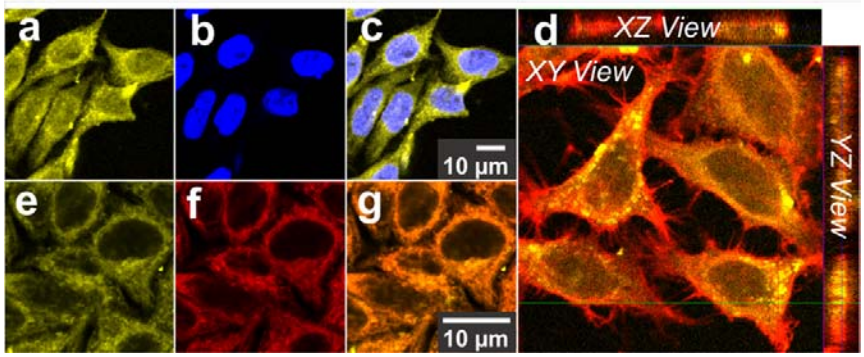

Fig. 6 Fluorescence confocal micrographs showing the distribution of compound **4** inside HeLa cells at concentration of 100 μM in less than 1% DMSO containing PBS as the incubation media. (a) and (e) **4**, (b) DAPI staining of nucleus, (c) overlay (a) and (b), (d) orthogonal view of the image showing **4** signal (yellow) coming from inside cytoplasmic region of the cells which is stained with Phalloidin Alexa Fluor® 647 (red), (f) ER-Tracker™ Red stains endoplasmic

reticulum, (g) overlay (e) and (f). The excitation wavelength for DAPI and compound **4** was 405 nm, while ER-Tracker™ Red and Phalloidin Alexa Fluor® 647 were excited at 594 and 633 nm, respectively.

In sharp contrast, incubation with compound **6** of HeLa cells under identical condition, resulted in no emission detected from the cells except of typical autofluorescence signal derived from NADH and FAD molecules[17] (see Fig S9, ESI). Even though at this stage it is still not clear if the compound was uptaken but the emission was quenched or not uptaken at all.

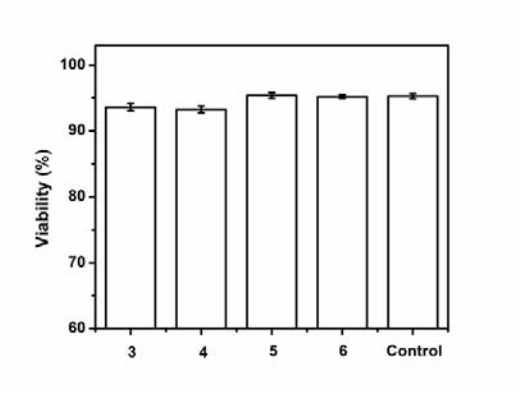

Fig. 7 Cellular viability studies after 1 hour incubation with different complexes at a concentration of 50 µM in <1% DMSO containing PBS.

Noteworthy, typical healthy cell shapes and no sign of apoptosis were observed during the experiments. Indeed, this observation neglecting any degree of toxicity governed by the presence of the compounds inside the cellular organelles. To further quantify such a finding, cellular viability assay based on electric current exclusion and pulse area analysis were performed by means of CASY® equipment and the results are depicted in Fig. 7. Interestingly, the number of viable cells after 1 hour incubation of four different complexes is found to be close to the control experiments, confirming the low cytotoxicity of the complexes and their suitability as efficient phosphorescent labelling probes to be used in cellular imaging applications.

Conclusions

Different glyco-conjugates based on luminescent dinuclear rhenium complexes have been synthetized using glucose or maltose derivatives and bio-orthogonal glyco-conjugation procedures. These new conjugates have been evaluated in terms of their optical properties and suitability as bio-imaging dyes in living cells. The conjugation with sugars increases the water solubility of the complexes and does not appear to perturb the nature of the complex excited state. Moreover, it affords an amphiphilic character to the resulting glyco-conjugates, allowing the formation of soft aggregates, which display higher photoluminescent quantum yield and longer excited state lifetime than the corresponding molecular complex.

Cellular internalization experiments on human cervical adenocarcinoma cells (HeLa) have shown that these glyco-conjugates have fascinating bio-imaging properties, i.e. high cell permeability, organelle selectivity, low cytotoxicity, fast internalization, and suitability as efficient phosphorescent probes to be used in cell imaging application.

Experimental

Supporting figures, and synthetic procedures, including NMR and high-resolution mass spectra, are described in the ESI.

Materials and methods

Chemicals were purchased by commercial sources and used without further purification, unless indicated otherwise. When anhydrous conditions were required, the reactions were performed in oven-dried glassware under nitrogen atmosphere. Anhydrous solvents were purchased by Sigma-Aldrich® with a content of water ≤0.005 %. THF was dried over Na/benzophenone and freshly distilled prior to use. Thin-layer chromatography (TLC) was performed on Silica Gel 60 F254 plates or RP-C18 Silica plates (Merck) with UV detection (254 nm and 365 nm) or using appropriate developing solutions. The Flash column chromatography was performed on silica gel 230-400 mesh (Merck), according with the procedure described in literature. Automated flash chromatography was perfomed on a Biotage® Isolera™ Prime system. NMR experiments were recorded on a Bruker AVANCE 400 MHz instrument at 298 K. Chemical shifts (δ) are reported in ppm downfield from TMS as internal standard, whereas coupling constants (J) are stated in Hz. The ^{1}H and ^{13}C-NMR resonances of compounds were assigned by the meaning of COSY and HSQC experiments. Mass spectra were recorded on Apex II ICR FTMS (ESI ionization-HRMS), Waters Micromass Q-TOF (ESI ionization-HRMS), ThermoFischer LCQ apparatus (ESI ionization) or Bruker Daltonics Microflex LT (MALDI-TOF apparatus). Specific optical rotation values were measured using a Perkin-Elmer 241, at 589 nm in a 1 mL cell. In the optimized Copper(I)-catalyzed Azide-Alkyne Cycloaddition (CuAAC) procedure, the starting materials and reagents were added to the reaction mixture as solid or as solution in water or THF. The water was degassed by bubbling with nitrogen and THF was freshly distilled. The reagents were added to the reaction vessel in the following order: multivalent scaffold (1 eq, solid or in THF), TBTA (0.2 eq, in THF), $CuSO_4{\cdot}5H_2O$ (0.1 eq, in H_2O), sodium ascorbate (0.4 eq, in H_2O) and finally the azide monovalent ligand (1.1 eq per each triple bond, solid or in H_2O). The final concentration of multivalent scaffold was around 20 mM in a mixture THF:H_2O (1:1) and the reaction was stirred overnight at room temperature under nitrogen

atmosphere, protected from light and monitored by mass spectrometry (MALDI-Tof) until the completion. When RP-C18 chromatography was required, the sample was loaded on C18 prepacked samplet and purified using Biotage system (column SNAP KP-C18-HS, gradient elution H_2O:MeOH). Finally the solvent was removed by lyophilization obtaining the final purified product.

Synthesis

$[ReCl(CO)_5]$, and complex **1** were prepared according to literature method.[18,11,16] Synthesis of 4-ethanoyl-5-ethyl-pyridazine was carried out according to a literature procedure,[14,19] involving as first step the synthesis of 1,2,4,5-tetrazine (from hydrazine hydrate and formamidine acetate) followed by its reaction with the alkyne.

Complex 2. A sample of $[ReCl(CO)_5]$ (117.1 mg, 0.324 mmol) was dissolved in toluene solution (20 mL) and treated with 0.5 eq of 4-ethanoyl-5-ethyl-pyridazine (24.3 mg, 0.162 mmol). The solution was heated at reflux temperature for three hours and then evaporated to dryness, giving a brownish solid. The desired product wa isolated as yellow solid from the crude on silica gel column chromatography using CH_2Cl_2:AcOEt 4:1 as eluent. IR (CH_2Cl_2) ν (CO): 2049 (m), 2033 (s), 1945 (s), 1914 (m) cm^{-1}. ^1H NMR (CD_2Cl_2, 300K, 400 MHz) δH (ppm) 9.65 (s, 1H, H3-pydz), 9.49 (s, 1H, H6-pydz), 4.06 (m, 2H), 3.10 (t, 2H), 2.97 (q, 2H), 1.42 (t, 3H). Elemental Anal. Calcd for $C_{14}H_{12}Cl_2N_2O_7Re_2$: C 22.02, H 1.58, N 3.67. Found: C 22.12, H 1.53, N 3.65.

Compound 9. To a solution of penta-*O*-acetyl-D-glucose (**8**) (1 g, 2.67 mmol, 1 eq) and 3-hexyn-1-ol (**7**) (365 µL, 3.2 mmol, 1.2 eq) in anhydrous DCM (22 mL), BF_3-Et_2O (507 µL, 4.0 mmol, 1.5 eq) was added at 0°C under nitrogen atmosphere. Then mixture was slowly allowed to warm and stirred for 4h at room temperature until the reaction was complete (TLC Hex:AcOEt 7:3 $Rf_{prod.}$= 0.26). Finally the reaction was quenched by addition of Et_3N (670 µL, 4.8 mmol, 1.8 eq), stirred for additional 15 min and concentrated under reduced pressure. The crude was purified by flash chromatography (hexane: AcOEt gradient elution) affording pure compound (9) (740 mg, 68 %, β-anomer). ^1H NMR (400 MHz, $CDCl_3$) δ 5.20 (t, $J_{3,2}$= 9.5 Hz, 1H, H_3), 5.08 (t, $J_{4,5}$ = 9.7 Hz, 1H, H4), 4.98 (dd, $J_{2,3}$ = 9.5 Hz, $J_{1,2}$ = 8.0 Hz, 1H, H2), 4.56 (d, $J_{1,2}$ = 8.0 Hz, 1H, H1), 4.26 (dd, $J_{6a,6b}$ = 12.3 Hz, $J_{6a,5}$ = 4.7 Hz, 1H, H6a), 4.13 (dd, $J_{6a,6b}$ = 12.3, $J_{6b,5}$ =2.4 Hz, 1H, H6b), 3.89 (dt, $J_{7a,7b}$ = 9.8, $J_{7a,8}$ = 7.0 Hz, 1H, H7a), 3.69 (ddd, $J_{5,4}$ = 9.9 Hz, $J_{5,6a}$ = 4.7 Hz, $J_{5,6b}$ = 2.4 Hz, 1H, H5), 3.62 (dt, $J_{7a,7b}$ = 9.8, $J_{7b,8}$ = 7.5 Hz, 1H, H7b), 2.43 (tt, $J_{8,7}$ = 7.1 Hz, $J_{8,11}$ = 2.3 Hz, 2H, H8), 2.18 – 2.10 (m, 2H, H11), 2.09 (s, 3H, AcO), 2.05 (s, 3H, AcO), 2.02 (s, 3H, AcO), 2.00 (s, 3H, AcO), 1.10 (t, $J_{12,11}$ = 7.5 Hz, 3H, H12). 13C NMR (100 MHz, $CDCl_3$) δ 170.85, 170.46, 169.54, 169.50 (CO), 100.95 (C1), 83.21, 75.35 (C9, C10), 72.94 (C3), 71.97 (C5), 71.33 (C2), 68.81 (C7), 68.53 (C4), 62.07 (C6), 20.90, 20.81, 20.78, 20.76 (AcO), 20.24 (C8), 14.29 (C12), 12.52 (C11). MS (ESI) m/z calculated for $[C_{20}H_{28}O_{10}Na]^+$: 451.16 found: 451.4 $[M+Na]^+$. $[\alpha]^D_{25}$= -17.85 (C=0.685, CH_3Cl).

Compound 10. A solution of compound (**9**) (740 mg, 1.73 mmol) in freshly distilled MeOH (31.5 mL) was treated with a solution of NaOMe (3.5 mL, 1 M in MeOH). The reaction was stirred at room temperature under nitrogen atmosphere monitoring the progress by TLC (hexane: AcOEt 1:1). After 1 h the reaction was complete. The mixture was diluted with MeOH and neutralized by addition of Amberlite IR 120-H^+ resin, then the beads was filtered off and washed with MeOH. Finally the solvent was removed under reduced pressure and the crude was purified by flash chromatography (DCM:MeOH 9:1) affording pure compound (**10**) (420 mg, 93 %). ^1H NMR (400 MHz, MeOD) δ 4.29 (d, $J_{1,2}$ = 7.8 Hz, 1H, H1), 3.98 – 3.81 (m, 2H, H6a, H7a), 3.72 – 3.56 (m, 2H, H6b, H7b), 3.37 – 3.32 (m, 1H, H3), 3.28 – 3.24 (m, 2H, H4, H5), 3.17 (dd, $J_{2,3}$ = 8.9, $J_{2,1}$ = 7.8 Hz, 1H, H2), 2.46 (tt, $J_{8,7}$ = 7.4, $J_{8,11}$ = 2.3 Hz, 2H, H8), 2.13 (qt, $J_{11,12}$ = 7.5, $J_{8,11}$ =2.3 Hz, 2H, H11), 1.09 (t, $J_{11,12}$ = 7.5 Hz, 3H, H12). ^{13}C NMR (100 MHz, MeOD) δ 104.36 (C1), 83.52, 78.01 (C3), 77.98 (C4), 76.61, 75.01 (C2), 71.57 (C5), 69.59 (C7), 62.71 (C6), 20.86 (C8), 14.64 (C12), 13.03 (C11); MS (ESI) m/z calculated for $[C_{12}H_{20}O_6Na]^+$: 283.27 found: 283.3 $[M+Na]^+$. $[\alpha]^D_{25}$: -35.2 (C = 0.481, MeOH).

Compound 11. Synthesis of glycosylated pyridazine was carried out according to a literature procedure [ref], involving as first step the synthesis of 1,2,4,5-tetrazine (from hydrazine hydrate and formamidine acetate) followed by its reaction with the functionalized alkyne **10** (Scheme 1) The crude was purified by RP-18 chromatography (H_2O:MeOH gradient elution) affording pure compound (**11**) (mg, 35% yield). ^1H NMR (400 MHz, MeOD) δ 9.07 (s, 1H, HAr), 8.96 (s, 1H, HAr), 4.31 (d, $J_{1,2}$ = 7.8 Hz, 1H, H1), 4.18 (dt, $J_{7a,7b}$ = 10.1, $J_{7a,8}$ = 6.5 Hz, 1H, H7a), 3.94 – 3.81 (m, 2H, H7b, H6a), 3.69 – 3.60 (m, 1H, H6b), 3.37 – 3.33 (m, 1H, H5), 3.26 (m, 2H, H3, H4), 3.15 (dd, $J_{2,3}$ = 9.1, $J_{1,2}$ = 7.8 Hz, 1H, H2), 3.08 (t, $J_{7,8}$ = 6.4 Hz, 2H, H8), 2.81 (q, $J_{11,12}$ = 7.6 Hz, 2H, H11), 1.29 (t, $J_{11,12}$ = 7.6, 3H, H12); ^{13}C NMR (100 MHz, MeOD) δ 153.58, 152.72 (CHAr), 144.85, 139.64 (CqAr), 104.42 (C1), 78.13, 78.05 (C4, C5), 75.00 (C2), 71.60 (C3), 69.01 (C7), 62.76 (C6), 30.56 (C8), 23.58 (C11), 14.22 (C12). MS (ESI) m/z calculated for $[C_{14}H_{22}N_2O_6Na]^+$: 337.32 found: 337.4 $[M+Na]^+$; $[\alpha]^D_{25}$: -16.01 (C = 0.316, MeOH).

Complex 3. The complex **3** (see Chart 3 for their structures and abbreviations) was prepared from $[ReCl(CO)_5]$, using the previously reported method. The crude was purified by RP-18 chromatography (H_2O:MeOH gradient elution) affording pure compound (**3**) (mg, 12% yield). ^1H NMR (400 MHz, MeOD) δ 9.84 (s, 1H, HAr), 9.74 (s, 1H, HAr), 4.32 (d, $J_{1,2}$ = 7.6 Hz, 1H, H1), 4.24 – 4.14 (m, 1H, H7a), 4.08 – 3.99 (m, 1H, H7b), 3.86 (dd, $J_{6a,6b}$ = 11.7, $J_{6a,5}$ = 2.3 Hz, 1H, H6a), 3.56 (dd, $J_{6a,6b}$ = 11.7, $J_{6b,5}$ = 6.8 Hz, 1H, H6b), 3.36 – 3.15 (m, 8H, H2, H3, H4, H5, H8), 3.00 (q, $J_{11,12}$ = 7.6 Hz, 2H, H11), 1.37 (t, $J_{11,12}$ = 7.6 Hz, 3H, H12); ^{13}C NMR (100 MHz, MeOD) δ 195.79, 191.96 (CO), 164.48, 163.16 (CAr), 151.05, 146.43 (C9, C10), 105.11 (C1), 78.37, 78.14 (C4, C5), 74.68, 71.74 (C2, C3), 69.05 (C7), 63.03 (C6), 31.32 (C8), 24.07 (C11), 13.88 (C12); MS (ESI) 949.2 $[M+Na]^+$, HRMS (ESI) m/z calculated for $[C_{20}H_{22}Cl_2N_2O_{12}Re_2Na]^+$: 948,95311 found: 948.95418 $[M+Na]^+$ (error: 1.1 ppm) ; $[\alpha]^D_{25}$: + 6.21 (C = 0.43, MeOH).

Formattato: Apice

Formattato: Apice

Compound 13 To a solution of 2-(2-Chloroethoxy)ethanol (**12**) (423 µL, 4 mmol, 1 eq) in water (5 mL), NaN_3 (782 mg, 12 mmol, 3eq) and NaI (60 mg, 0.4 mmol, 0.1 eq) were added. The reaction mixture was stirred at 60°C for 96 h. The mixture was saturated with NaCl and extracted with DCM (3 x 10 mL), the organic phase was dried over Na_2SO_4, filtered, concentrated under nitrogen flow and used without further purification.

Compound 14. To a solution of compound (**13**) (4 mmol, 1eq) in DCM (25mL), TsCl (1.15 g, 6 mmol, 1.5 eq) and then Et_3N (1.7 mL, 12 mmol, 3 eq) were added under nitrogen at 0 °C, then the mixture was stirred at r.t. for 3h. The crude solution was washed with saturated $NaHCO_3$ (3 x 20 mL) and brine (20 mL), dried on anhydrous Na_2SO_4, filtered and evaporated under reduced pressure. Flash cromatography purification (Hex: AcOEt gradient elution) giving pure compound (**14**) (1.09 g, 80 % yield). ^{1}H NMR (400 MHz, $CDCl_3$) δ 7.80 (d, J_{AB} = 8.2 Hz, 2H, AA'BB', Ar-HAA'), 7.35 (d, J_{AB} = 8.2 Hz, 2H, AA'BB', Ar-HBB'), 4.25 – 4.08 (m, 2H, H4), 3.76 – 3.64 (m, 2H, H3), 3.64 – 3.57 (m, 2H, H2), 3.32 (t, $J_{1,2}$ = 5.0 Hz, 2H, H1), 2.45 (s, 3H, Me); ^{13}C NMR (100 MHz, $CDCl_3$) δ 145.05, 133.03 (Cq), 129.99, 128.12 (CHAr), 70.31 (C2), 69.25 (C4), 68.83 (C3), 50.76 (C1), 21.78 (Me); MS (ESI) m/z calculated for $[C_{11}H_{15}N_3O_4SNa]^+$: 308.06, found: 308.1 $[M+Na]^+$.

***N*-Boc-*N*-methylhydroxylamine**. To solution of N-methylhydroxylamine hydrochloride (630 mg, 7.54 mmol, 1 eq) in dry DCM (36 mL), di-tert-butyl dicarbonate (1.3 g, 6.03 mmol, 0.8 eq) was added, then the mixture was treated with Et_3N (1 mL, 7.54 mmol, 1 eq) and stirred at r.t. under nitrogen atmosphere for 4 hours. Finally, the crude solution was washed with $NaHSO_4$ 0.1M (3 x 25 mL) and brine (3 x 25 mL). The organic phase was dried on anhydrous Na_2SO_4, filtered and evaporated under reduced pressure giving pure *N*-Boc-*N*-methylhydroxylamine (583 mg, 52% yield). ^{1}H NMR (400 MHz, $CDCl_3$) δ 6.68 (bs, 1H, OH), 3.15 (s, 3H, NMe), 1.49 (s, 9H, tBu).

Compound 15 To a solution of *N*-Boc-*N*-methylhydroxylamine (360 mg, 2.45 mmol, 1.4 eq) in dry THF (2 mL), DBU (393 µL, 2.63 mmol, 1.5 eq) and a solution of compound **14** (500 mg, 1.75 mmol, 1 eq) in dry THF (1.5 mL) were added. Then the mixture was stirred and left under flow of nitrogen until the solvent was removed, then the neat reaction was stirred overnight at room temperature. The crude was suspended in AcOEt (30 mL) and the organic phase was washed with $NaHSO_4$ 0.1 M (3 x 10 mL), NaOH 0.1 M (3 x 10 mL) and brine (10 mL), then dried on anhydrous Na_2SO_4 and filtered. The evaporation of the solvent under reduced pressure giving pure compound (**15**) (400 mg, 88% yield). ^{1}H NMR (400 MHz, $CDCl_3$) δ 4.05 – 3.97 (m, 2H, H4), 3.74 – 3.61 (m, 4H, H2, H3), 3.43 – 3.34 (m, 2H, H1), 3.10 (s, 3H, Me), 1.47 (s, 9H, tBu). ^{13}C NMR (100 MHz, $CDCl_3$) δ 157.11 (CO), 81.44 (Cq), 73.68 (C1), 70.12, 68.92 (C2, C3), 50.83 (C1), 36.91 (NMe), 28.38 (tBu). MS (ESI) m/z calculated for $[C_{10}H_{20}N_4O_4Na]^+$: 283.13, found: 283.1 $[M+Na]^+$.

Compound 16. To a solution of compound (**15**) (60 mg, 0.23 mmol, 1 eq) in DCM (2 mL), PPh_3 (113 mg, 0.43 mmol, 1.9 eq), Na_2CO_3 (46 mg, 0.23 mmol, 1 eq) and H_2O (400 µL) were added, then the reaction mixture was vigourously stirred at r.t. overnight. The solvents was removed under reduced pressure and the crude was purified by flash chromatography (eluent DCM:MeOH 9:1 + 1% NH_3 7N in MeOH) obtaining pure compound (**16**) (46 mg, 85% yield) as a yellowish oil. ^{1}H NMR (400 MHz, MeOD) δ 4.02 – 3.97 (m, 2H, H4), 3.69 – 3.63 (m, 2H, H3), 3.53 (t, *J* = 5.3 Hz, 2H, H2), 3.11 (s, 3H, NMe), 2.79 (t, $J_{1,2}$ = 5.3 Hz, 2H, H1), 1.49 (s, 9H, tBu). ^{13}C NMR (100 MHz, MeOD) δ 158.55 (CO), 82.73 (Cq), 74.63 (C4), 73.38 (C2), 69.57 (C3), 42.08 (C1), 37.04 (NMe), 28.52 (tBu); MS (ESI) m/z calculated for $[C_{10}H_{23}N_2O_4]^+$: 235.30, found: 235.1 $[M+H]^+$.

Compound 17a. To a solution of compound (**1**) (48 mg, 62 µmol, 1.1 eq) in DCM dry (2.5% DMA dry) (2 mL + 70 µL), HATU (32 mg, 85 µmol, 1.5 eq) and then freshly distilled DIPEA (29 µL, 17 µmol, 3 eq) were added under nitrogen atmosphere. After 15 min a solution of compound (**16**) (13 mg, 56 µmol, 1 eq) in DCM dry (600 µL) were added and the reaction was stirred at r.t. under nitrogen for 1 h. The crude was coevaporated with toluene and $CHCl_3$ and purified by flash chromatography (hexane:AcOEt gradient elution) obtaining of pure compound (**17a**) (47 mg, 72% yield). ^{1}H NMR (400 MHz, $CDCl_3$) δ 9.67 – 9.55 (m, 2H, H-10, H11), 8.00 (dd, $J_{9,10}$ = 5.9, J9,11 = 2.3 Hz, 1H, H9), 7.10 (bt, 1H, NH), 4.01 – 3.94 (m, 2H, H1), 3.70 – 3.62 (m, 2H, H2), 3.62 – 3.56 (m, 2H, H3), 3.42 (m, 2H, H4), 3.13 (s, 3H, NMe), 2.98 (t, $J_{7,6}$ = 7.5 Hz, 2H, H7), 2.44 – 2.37 (m, 2H, H5), 2.20 – 2.10 (m, 2H, H6), 1.47 (s, 9H, OtBu); ^{13}C NMR (100 MHz, $CDCl_3$) δ 193.62, 193.46, 190.66 (CORe), 171.63 (CONH), 163.02, 161.22 (C10, C11), 157.04 (OCON), 149.01 (C8), 132.00 (C9), 81.90 (Cq), 73.24 (C1), 69.54 (C3), 67.99 (C2), 39.12 (C4), 36.87 (NMe), 34.16 (C5), 31.94 (C7), 28.41 (tBu), 25.13 (C6); MS (ESI) m/z calculated for $[C_{24}H_{30}Cl_2N_4O_{11}Re_2Na]^+$: 1017.02, found: 1017.2 $[M+Na]^+$ and 993.5 $[M-H]^-$.

Compound 17b. A solution of compound (**17a**) (47 mg, 47 µmol, 1 eq) in dry DCM (2.4 mL) was treated with TFA (181 µL, 2.36 mmol, 50 eq) under nitrogen atmosphere at 0°C, then the mixture was stirred at room temperature for 1 hour until the reaction was complete (TLC AcOEt:MeOH 9:1 $Rf_{prod.}$= 0.28). The crude was diluted with $CHCl_3$ and coevaporated with toluene (3x) and $CHCl_3$ (3x) affording compound (**17b**) in quantitative yield that was used without further purification. ^{1}H NMR (400 MHz, MeOD) δ 9.96 (dd, $J_{9,11}$ = 2.3 Hz, $J_{10,11}$ = 0.9 Hz, 1H, H11), 9.88 (dd, $J_{9,10}$ = 5.9 Hz, $J_{10,11}$ = 0.9 Hz, 1H, H10), 8.11 (dd, $J_{9,10}$ = 5.9 Hz, $J_{9,11}$ = 2.3 Hz, 1H, H9), 4.24 – 4.14 (m, 2H, H1), 3.80 – 3.71 (m, 2H, H2), 3.56 (t, $J_{3,4}$ = 5.5 Hz, 2H, H3), 3.37 (t, $J_{3,4}$ = 5.5 Hz, 2H, H4), 3.00 – 2.94 (m, 5H, NMe, H5), 2.35 (t, $J_{6,7}$ = 7.1 Hz, 2H, H7), 2.15 – 2.03 (m, 2H, H6). ^{13}C NMR (100 MHz, MeOD) δ 195.63, 191.77 (CO), 175.33 (CONH), 165.01 (C11), 163.12 (C10), 151.16 (C8), 133.64 (C9), 74.27 (C1), 71.38 (C3), 70.52 (C2), 40.25 (C4), 36.70 (NMe), 35.71 (C7), 32.73 (C5), 26.24 (C6).

Complex 4. To a solution of compound (**17b**) (23 mg, 22.8 µmol, 1 eq) and D-glucose (12 mg, 69 µmol, 3 eq) in dry MeOH (230 µL), glacial AcOH (33 µL, 0.57 mmol, 25 eq) was added then the mixture was stirred at r.t. overnight. The crude mixture was directly loaded on C-18 column and purified by RP-18 cromathography (H_2O:MeOH) gradient elution affording pure compound (**4**) (15 mg, 62 % yield). ^{1}H NMR (400 MHz, MeOD) δ 9.99 (dd, $J_{15,17}$ = 2.3 Hz, J16,17 = 0.9 Hz, 1H, H17), 9.88 (dd, $J_{15,16}$ = 5.9 Hz, $J_{16,17}$ = 0.9 Hz, 1H, H16), 8.14 (dd, $J_{15,16}$ = 5.9 Hz, $J_{15,17}$ = 2.3 Hz, 1H, H15), 8.02 (bt, $J_{NH,10}$ = 5.7 Hz, 1H, NH), 3.99 (d, $J_{1,2}$ = 8.9 Hz, 1H, H1), 3.92 (t, $J_{7,8}$ = 4.5 Hz, 2H, H7), 3.86 (dd, $J_{6a,6b}$ = 12.0 Hz, $J_{5,6a}$ = 2.2 Hz, 1H, H6a), 3.70 (dd, $J_{6a,6b}$ = 12.0, $J_{5,6b}$ = 5.1 Hz, 1H, H6b), 3.67 – 3.60 (m, 2H, H8), 3.55 (t, $J_{9,10}$ = 5.2 Hz, 2H, H9), 3.49 (t, $J_{1,2}$ = 8.9 Hz, 1H, H2), 3.42 – 3.32 (m, 4H, H3, H4, H10), 3.23 (ddd, $J_{4,5}$ = 9.5 Hz, $J_{5,6b}$ = 5.1 Hz, $J_{5,6a}$ = 2.2 Hz, 1H, H5), 3.02 – 2.94 (m, 2H, H11), 2.74 (s, 3H, NMe), 2.42 – 2.32 (m, 2H, H13), 2.15 – 2.02 (m, 2H, H12). ^{13}C NMR (100 MHz, MeOD) δ 195.68, 191.78 (CO), 174.98 (CONH), 165.04, 163.15 (C16, C17), 151.28 (Cq), 133.69 (C15), 95.45 (C1), 79.61 (C4), 79.25 (C5), 73.04 (C7), 71.61 (C2), 71.27 (C3), 70.39 (C9), 70.16 (C8), 62.79 (C6), 40.44 (C10), 39.23 (NMe), 35.75 (C13), 32.69 (C11), 26.35 (C12). HRMS (ESI) m/z calculated for $[C_{25}H_{32}Cl_2N_4O_{14}Re_2Na]^+$: 1079.02751 found: 1079.02718 $[M+Na]^+$ (error: -0.3 ppm) ; $[\alpha]^D_{25}$: -3.03 (C = 0.515, MeOH).

Complex 5. To a solution of compound (**17b**) (23 mg, 22.8 µmol, 1 eq) and D-maltose (25 mg, 69 µmol, 3 eq) in dry MeOH (230 µL), glacial AcOH (33 µL, 0.57 mmol, 25 eq) was added then the mixture was stirred overnight at room temperature. The crude mixture was directly loaded on C-18 column and purified by RP-18 cromathography (H_2O: MeOH gradient elution) affording pure compound (5) (15 mg, 62 % yield). ^{1}H NMR (400 MHz, MeOD) δ 9.99 (dd, $J_{15,17}$ = 2.3 Hz, $J_{16,17}$ = 0.9 Hz, 1H, H17), 9.88 (dd, $J_{15,16}$ = 5.9 Hz, J16,17 = 0.9 Hz, 1H, H16), 8.15 (dd, $J_{15,16}$ = 5.9, $J_{15,17}$ = 2.3 Hz, 1H, H15), 8.04 (bt, $J_{NH,10}$ = 5.4 Hz, 1H, NH), 5.16 (d, $J_{1',2'}$ = 3.8 Hz, 1H, H1'), 4.01 (d, $J_{1,2}$ = 8.9 Hz, 1H, H1), 3.92 (t, $J_{7,8}$ = 4.4 Hz, 2H, H7), 3.89 – 3.79 (m, 2H, H6a, H6'ab), 3.72 – 3.52 (m, 10H, H8, H6b, H2, H3, H3', H4, H4', H9), 3.45 (dd, $J_{2',3'}$ = 9.7, $J_{1',2'}$ 3.8 Hz, 1H, H2'), 3.41 – 3.33 (m, 3H, H10, H5), 3.29 – 3.23 (m, 2H, H5'), 3.01 – 2.94 (m, 2H, H11), 2.75 (s, 3H, NMe), 2.38 (t, $J_{12,13}$ = 7.1 Hz, 2H, H13), 2.14 – 2.04 (m, 2H, H12). ^{13}C NMR (100 MHz, MeOD) δ 195.67, 195.60, 191.78, 191.71 (CO), 174.98 (CONH), 165.03, 163.17 (C16, C17), 151.27 (C14), 133.75 (C15), 102.93 (C1), 95.38 (C1'), 81.06, 78.96, 78.21, 75.09, 74.80, 74.19, 73.06 (C7), 71.47, 71.19, 70.41 (C8), 70.16 (C9), 62.72 (C6), 62.28 (C6'), 40.43 (C10), 39.38 (NMe), 35.77 (C13), 32.70 (C11), 26.38 (C12). HRMS (ESI) m/z calculated for $[C_{31}H_{48}Cl_2N_4O_{19}Re_2Na]^+$: 1241.08057 found 1241.08278 $[M+Na]^+$ (error: 1.8 ppm). $[\alpha]^D_{25}$: + 15.54 (C = 0.605, MeOH)

Compound 6. To a solution of compound (**1**) (18 mg, 23 µmol, 1.2 eq) and HATU (11 mg, 29 µmol, 1.5 eq) in DMA dry (600 µL), freshly distilled DIPEA (10 µL, 57 µmol, 3 eq) were added under nitrogen atmosphere. After 15 min a solution of compound (**21**) (24 mg, 19 µmol, 1 eq) in DMA dry (400 µL) were added and the reaction was stirred at r.t. under nitrogen for 1 h. The crude was directly loaded on C-18 column and purified by RP-18 chromatography (H_2O:MeOH gradient elution) obtaining of pure compound (**6**) (26 mg, 68% yield). ^{1}H NMR (400 MHz, MeOD) δ 10.00 (dd, *J* = 2.2, 0.9 Hz, 1H, H27), 9.89 (dd, *J* = 5.9, 0.9 Hz, 1H, H26), 8.14 (dd, *J* = 5.9, 2.3 Hz, 1H, H25), 8.03 (s, *J* = 6.9 Hz, 3H, H11), 4.60 – 4.55 (m, 6H, H10), 4.53 (s, 6H, H13), 4.29 (d, *J* = 7.8 Hz, 3H, H1), 4.01 – 3.94 (m, 3H, H7a), 3.93 – 3.89 (m, 6H, H9), 3.89 – 3.85 (m, 3H, H6a), 3.74 – 3.63 (m, 14H, H6b, H7b, H8, H19), 3.56 – 3.48 (m, 4H, H17, H18), 3.46 (s, 6H, H14), 3.42 (s, 2H, H16), 3.39 – 3.36 (m, 3H, H3), 3.35 – 3.32 (m, 2H, H20), 3.30 – 3.25 (m, 6H, H4, H5), 3.20 (dd, *J* = 9.1, 7.8 Hz, 3H, H2), 3.02 – 2.91 (m, 2H, H21), 2.35 (t, *J* = 7.1 Hz, 2H, H23), 2.12 – 2.02 (m, 2H, H22); 13C NMR (100 MHz, MeOD) δ 195.69, 195.61, 191.79, 191.71 (ReCO), 174.92 (CONH), 165.09, 163.20 (C26, C27), 151.28 (C24), 146.02 (C12), 133.75 (C25), 125.99 (C11), 104.48 (C1), 78.05, 78.01 (C3, C5), 75.11 (C2), 72.18 (C17), 71.64 (C4), 71.38 (C8), 71.25 (C18), 70.81 (C16), 70.51 (C19), 70.34 (C9), 70.03 (C14), 69.81 (C7), 65.32 (C13), 62.77 (C6), 51.35 (C10), 46.58 (C15), 40.49 (C20), 35.75 (C22), 32.69 (C21), 26.31 (C22); HRMS (ESI-Qtof) *m/z* calculated for $[C_{62}H_{92}Cl_2N_{12}O_{33}Re_2Na_2]^{2+}$: 1011.2061 found: 1011.1946 $[M+2Na]^{2+}$; (error: 11 ppm); $[\alpha]_D^{25}$: -12.43 (C = 0.725, MeOH).

Photophysical characterization

Steady-state measurements. Absorption spectra were measured on a double-beam Shimadzu UV-3600 UV-Vis-NIR spectrophotometer and baseline corrected. Steady-state emission spectra were recorded on a HORIBA Jobin-Yvon IBH FL-322 Fluorolog 3 spectrometer equipped with a 450 W xenon arc lamp and a TBX-4-X single-photon-counting as excitation source and detector, respectively. Emission spectra were corrected for source intensity (lamp and grating) and emission spectral response (detector and grating) by standard correction curves. Photoluminescence quantum yields for samples were measured with a Hamamatsu Photonics absolute PL quantum yield measurement system (C9920-02) equipped with a L9799-01 CW Xenon light source (150 W), monochromator, C7473 photonic multichannel analyzer, integrating sphere and employing U6039-05 PLQY measurement software (Hamamatsu Photonics, Ltd., Shizuoka, Japan).

Lifetime measurements. Time-resolved measurements were performed using either the time-correlated single-photon counting (TCSPC) electronics PicoHarp300 or the Multi Channel Scaling (MCS) electronics NanoHarp 250 of the PicoQuant FluoTime 300 (PicoQuant GmbH, Germany), equipped with a PDL 820 laser pulse driver. A pulsed laser diode LDH-P-C-405 (λ_{ex} = 405 nm, pulse FWHM <70 ps, repetition rate 200 kHz – 40 MHz) was used to excite the sample and mounted directly on the sample chamber at 90°. The photons were collected by a PMA-C-192 photomultiplier (PMT) single-photon-counting detector. The data were acquired by using the commercially available software EasyTau (PicoQuant GmbH, Germany), while data analysis was performed using the commercially available software FluoFit (PicoQuant GmbH, Germany). The quality of the fit was assessed by minimizing the reduced χ^2 function and by visual inspection of the weighted residuals. For multi-exponential decays, the intensity, namely *I(t)*,

has been assumed to decay as the sum of individual single exponential decays (Eqn. 1):

$$I(t) = \sum_{i=1}^{n} \alpha_i exp\left(-\frac{t}{\tau_i}\right) \quad (1)$$

where τ_i are the decay times and α_i are the amplitude of the components at t = 0. In the tables, the percentages to the pre-exponential factors, α_i, are listed upon normalization.

Fluorescence confocal microscopy

The experiments were carried out by incubating approximately 50,000 HeLa cells with various concentrations of compound solutions (25-100 μM in less than 1% v/v of DMSO/Phosphate Buffer Saline, PBS) for 1h at normal biological conditions (37 °C and 5% CO_2). After the incubation, stained cells were imaged directly using a fluorescence confocal microscopy setup. All of the fluorescence images were taken by Zeiss LSM 710 confocal microscope set up with 63x magnification, numerical aperture, NA, 1.3 of Zeiss LCI Plan-NEOFLUAR water immersion objective lens (Zeiss GmbH) equipped with a spectrometer. Image acquisition was directly performed by exciting the samples using a continuous wave (cw) laser at 405 nm. The emission of the complexes was collected in the range from 540 to 720 nm and also scanned in lambda-mode (for acquiring the emission spectra). For co-localization experiments, the samples priory co-stained with different dyes, DAPI (excitation/emission wavelength: 358 nm/461 nm), ER Tracker Red (excitation/emission wavelength: 587 nm/615 nm), and Alexa Fluor® 647 Phalloidin (excitation/emission wavelength: 650 nm/668 nm) were excited independently at 405, 594 and 633 nm, and the emission signals were collected according to their corresponding emission profiles. All image processing was performed by using Zen 2011 software (Zeiss GmbH). False colour images were adjusted to better distinguish different complexes and complexes from cellular organelles.

Cell culture

All materials for cell culture were purchased from Gibco. Human cervical carcinoma, HeLa cells were cultured inside media containing 88% Dulbecco's Modified Eagle Medium (DMEM), 10% Fetal Bovine Serum (FBS), 1% Penicillin-Streptomycin and 1% L-Glutamine 200 mM under 37°C and 5% of CO_2 condition for 48 hours until reaching 70 to 80% cell confluency. Subsequently, the cells were washed twice with Phosphate Buffer Solution (PBS, Gibco), trypsinated and approximately 50,000 cells were reseeded on the monolayer glass cover slip inside six-well plate culture dish and glass bottom dishes (MatTek). Fresh culture media (2 mL) was added gently and cells were overnight grown.

Rhenium complexes incubation

The culture media was removed and 2 mL of new staining solution containing the corresponding Rhenium complexes (50 μM in less than 1% DMSO containing PBS) were gently added onto cells. After incubation at 37°C for 1 hour, the incubating media was removed and the cell layer on glass cover slips was gently washed (three times) with PBS and fixed with 4% paraformaldehyde (PFA) in PBS solution for 10 min.

Kinetic of internalization

The culture media of live cells grown onto glass bottom dishes was removed and 2 mL of complex staining solution (100 μM in less than 1% DMSO containing PBS) was added. The cells were subsequently imaged by fluorescence confocal microscopy setup for ten-minutes acquisition time for a total duration of 60 minutes.

Organelle staining

Cell layer was washed twice with PBS and kept in 0.1% Triton X-100 (Sigma Aldrich) in PBS for 5 minutes and afterwards in 1% bovine serum albumin, BSA (Sigma Aldrich), in PBS for 20 min. The cell layer on glass cover slip was stained with Phalloidin Alexa Fluor® 647 (Invitrogen), for f-actin/membrane staining, for 20 min, in the dark at room temperature, and washed two times with PBS. For visualizing nuclear region, cell nucleus was stained with 4',6-diamidino-2-phenylindole carboxamidine (DAPI) and washed twice with PBS. For case of 4, ER Tracker Red dye (Invitrogen) was added to visualize Endoplasmic Reticulum. The cover slips were mounted onto glass slides for microscopy measurements.

Cell viability studies

Cellular viability was measured by an automatic cell counter CASY (Roche Innovatis AG, Bielefeld, Germany). Approximately 50,000 cells were grown in 2 ml of culture media inside 6 well plates at 37oC, 5 % CO2 environment for 48 hours. Culture media was removed and replaced by 1 ml staining solution of complex **2**, **3**, **4**, and **5** (50 μM in less than 1% DMSO in PBS). Subsequently after 1 hour of incubation, the staining solution were removed to Eppendorf tubes and 0.5 ml of trypsin were added. To detach the cell from the surface of the plate, cells were incubated for 5 minutes in the same condition explained before. Subsequently, 0.5 ml of PBS was added to neutralize trypsin. Cell suspensions together with first solutions collected were removed into Eppendorf tube. 100 μl of the cell suspension was dissolved in 10 ml of CASY ton solution and measurement was performed. The positive control of cells grown without complexes was also performed. All experiments were repeated 3 times.

Acknowledgements

Author contribution

A.P., A.A., D.S. contributed equally to the work as follows: A.P. planned and performed the synthesis of all the compounds and of the complexes, supervised by A.B.; A.A. provided the spectroscopic and photophysical characterization of the conjugates, supervised by M.M.; D.S. performed cellular uptake experiments and acquired the confocal microscope images, all supervised by L.D.C.

M.P., M.M., A.P. and A.B. planned the experiments, analysed and discussed the data and wrote the paper.

Notes and references

1 (a) B. Imperiali, *J. Am. Chem. Soc.* 2012, **134**, 17835-17839; (b) W. H. Kim, J. Lee, D.-W. Jung, D. R. Williams, *Sensors* 2012, **12**, 5005-5027.

2 (a) G. Jaouen, Bioorganometallics II, Ed.; Wiley-VCH: Weinheim, Germany, 2015 ; (b) F.L., Thorp-Greenwood, M. P. Coogan, L. Mishra, N.Kumari, G. Rai, S. Saripella, *New J. Chem.*, 2012, **36**, 64–72; (c) Q. Zhao, C. Huang, F. Li, *Chem. Soc. Rev.,* 2011, **40**, 2508–2524; (d) F. L. Thorp-Greenwood, R. G. Balasingham, M. P. Coogan, *J. Organomet. Chem.*, 2012, **714**, 12-21

3 (a) V. Fernández-Moreira, F. L. Thorp-Greenwood, M. P. Coogan, *Chem. Commun.*, 2010, **46**, 186–202. (b) E. Baggaleya, J. A. Weinsteina, J. A. Gareth William, *Coord. Chem. Rev.*, 2012, **256**, 1762– 1785.

4 (a) M. Gottschaldt, U. S. Schubert , S. Rau, S. Yano, J.G. Vos, T. Kroll, J. Clement, I. Hilger, *ChemBioChem* 2010, **11**, 649-652. (b) D. Grunstein, M. Maglinao, R. Kikkeri, M. Collot, K. Barylyuk, B. Lepenies, F. Kamena, R. Zenobi, P. H. Seeberger, *J. Am. Chem. Soc.* 2011, **133**, 13957-13966. (c) R. Kikkeri, X. Liu, A. Adibekian, Y. –H. Tsai, P. H. Seeberger *Chem. Commun*., 2010, **46**, 2197–2199. (d) T. Okada, T. Makino, N. Minoura, *Bioconjugate Chem*. 2009, **20**, 1296–1298.

5 (a) L. Hua-Wei, K. Y. Zhang, W. H.-T. Law, K. K.-W. Lo, *Organometallics* 2010, **29**, 3474-3476. (b) M.-J. Li, P. Jiao, W. He, C. Yi, C. –W. Li, X. Chen, G.-N. Chen, M. Yang, *Eur. J. Inorg. Chem.* 2011, **2**, 197-200. (c) W. H.-T. Law, L. C.-C. Lee, M.-W. Louie, H.-W. Liu, T. W.-H. Ang, K. K.-W. Lo, *Inorg. Chem.* 2013, **52**, 13029-13041.

6 D.-L. Ma, T. Y.-T. Shum, F. Zhang, C.-M. Che, M. Yang, *Chem.Commun.* 2005, 4675 – 4677.

7 S. R. Banerjee, J. W. Babich, J. Zubieta, *Inorganica Chimica Acta* 2006, **359**, 1603–1612; (b) S. R. Bayly, C. L. Fisher, T. Storr, M. J. Adam, C. Orvig, *Bioconjugate Chem.* 2004, **15**, 923-926. (c) T. Storr, M. Obata, C. L. Fisher, S. R. Bayly, D. E. Green, I. BrudziÇska, Y. Mikata, B. O. Patrick, M. J. Adam, S. Yano, C. Orvig, , *Chem. Eur. J.* 2005, **11**, 195 – 203; (d) J. Petrig, R. Schibli, C. Dumas, R. Alberto, P. A. Schubiger, *Chem. Eur. J.* 2001, **7**, 1868-1973; (e) T. Storr, C. L. Fisher, Y. Mikata, S. Yano, M. J. Adam C. Orvig, , *Dalton Trans.,* 2005, 654-655; (f) T. Storr, Y. Sugai, C. A. Barta, Y. Mikata, M. J. Adam, S. Yano, C. Orvig, *Inorg. Chem.* 2005, **44**, 2698-2705. (g) C. L. Ferreira, C. B. Ewart, S. R. Bayly, B. O. Patrick, J. Steele, M. J. Adam, C. Orvig, , *Inorg. Chem.* 2006, **45**, 6979-6987. (h) T. L. Mindt, H. Struthers, L. Brans, T. Anguelov, C. Schweinsberg, V. Maes, D. Tourwe´, R. Schibli, , *J. Am. Chem. Soc.* 2006, **128**, 15096-15097.

8 (a) Y. Mikata, K. Takahashi, Y. Noguchi, M. Naemura, A. Ugai, S. Itami, K. Yasuda, S. Tamotsu, T. Matsuo, T. Storr, *Eur. J. Inorg. Chem*. 2012, **2**, 217–225 (b) M.-W. Louie, H.-W. Liu, M. Ho.-C. Lam, Y.-W. Lam, K. K.-W. Lo, *Chem. Eur. J*. 2011, **17**, 8304 – 8308. (c) K. Y. Zhang, K. K.-S. Tso, M.-W. Louie, H.-W. Liu, K. K.-W. Lo, *Organometallics* 2013, **32**, 5098−5102.

9 (a) D. Donghi, G. D'Alfonso, M. Mauro, M. Panigati, P. Mercandelli, A. Sironi, P. Mussini and L. D'Alfonso, *Inorg. Chem.*, 2008, **28**, 4243–4255; (b) M. Panigati, M. Mauro, D. Donghi, P. Mercandelli, P. Mussini, L. De Cola, G. D'Alfonso, *Coord. Chem. Rev*., 2012, **256**, 1621–1643.

10 (a) M. Mauro, M.; E. Quartapelle Procopio, Y. Sun, C. H. Chien, D. Donghi, M. Panigati, P. Mercandelli, P. Mussini, G. D'Alfonso, L. De Cola, *Adv. Funct. Mater*., 2009, **19**, 2607−2614; (b) M. Mauro, C.-H. Yang, C.-Y. Shin, M. Panigati, C.-H. Chang, G. D'Alfonso, L. De Cola, *Adv. Mater*., 2012, **24**, 2054−2058.

11 (a) E. Ferri, D. Donghi, M. Panigati, G. Prencipe, L. D'Alfonso, I. Zanoni, C. Baldoli, S. Maiorana, G. D'Alfonso, E. Licandro, *Chem. Commun*., 2010, **46**, 6255–6257; (b) C. Mari, M. Panigati, L. D'Alfonso, I. Zanoni, D. Donghi, L. Sironi, M. Collini, S. Maiorana, C. Baldoli, G. D'Alfonso, E. Licandro, *Organometallics* 2012, **31**, 5918-5928.

12 A. J. Amoroso, M. P. Coogan, J. E. Dunne, V. Fernandez-Moreira, J. B. Hess, A. J. Hayes, D. Lloyd, C. Millet, S. J. A. Pope, C. Williams, *Chem. Commun.* 2007, **29**, 3066-3068

13 (a) B. R. Griffith, J. M. Langenhan, J. S. Thorson, *Current Opinion in Biotechnology* 2005, **16**, 622-630. (b) J. M. Langenhan, B. R. Griffith, J. S. Thorson, *J. Nat. Prod.* 2005, **68** , 1696-1711.

14 J. Sauer, D. K. Heldmann, J. Hetzenegger, J. Krauthan, H. Sichert ,J. Schuster, *Eur. J. Org. Chem*., 1998, 2885–2896.

15 a) F. Peri, P. Dumy, M. Mutter, *Tetrahedron* 1998, **54**, 12269-12278. b) A. Palmioli, E. Sacco, S. Abraham, C. J. Thomas, A. D. Domizio, L. D. Gioia, V. Gaponenko, M. Vanoni and F. Peri, Bioorganic & Medicinal Chemistry Letters, 2009, **19**, 4217-4222. c) E. Sacco, S. J. Abraham, A. Palmioli, G. Damore, A. Bargna, E. Mazzoleni, V. Gaponenko, M. Vanoni and F. Peri, MedChemComm, 2011, **2**, 396-401.

16 C. Cebrián, M. Natali, D. Villa, M. Panigati, M. Mauro, G. D'Alfonso, L. De Cola, *Nanoscale*, 2015, **7**, 12000-12009.

17 a) H. Andersson, T. Baechi, M. Hoechl and C. Richter, *J. Microsc.*, 1998, **191**, 1–7; b) J. E. Aubin, J. *Histochem. Cytochem.*, 1979, **27**, 36–43.

18 S. P. Schmidt, W. C Trogler, F. Basolo, *Inorg. Synth.* 1985, **23**, 41.